

# Influence of the zeolite structure, in Mo/alumina-zeolite catalysts, on the hydroconversion of a model mixture of n-heptane-methylcyclohexane-toluene

Horacio González<sup>1,2</sup>, Jorge Ramírez<sup>2</sup>, Aída Gutiérrez,<sup>2</sup> Javier Lara<sup>1</sup>, José Luis Rico<sup>1</sup>

<sup>1</sup>Facultad de Ingeniería Química, Universidad Michoacana de San Nicolás de Hidalgo, Edificio M, Cd. Universitaria, 58060, Morelia, Michoacán, México. Tel. (443) 32735 84  
Email: [hogoro@zeus.umich.mx](mailto:hogoro@zeus.umich.mx)

<sup>2</sup>UNICAT, Dpto. de Ingeniería Química, Facultad de Química, U.N.A.M., Cd. Universitaria, 04510, México D.F., Tel.-Fax: 5622 53 66,

## Abstract

The hydroconversion of a n-heptane (62 mol-%)-methylcyclohexane (11 mol-%)-toluene (27 mol-%) model mixture was carried out over Mo(3 wt-%)/alumina-zeolite(20 wt-%) catalysts under the following operating conditions: temperature: 523-688 K, pressure:  $2.8 \times 10^6$  Pa, LHSV:  $1-10 \text{ h}^{-1}$  and  $\text{H}_2$ /hydrocarbon molar ratio: 2. It is well-known that the performance of Metal/zeolite hydroconversion catalysts depends on the shape selectivity properties of the zeolite, which in turn could modify the selectivity and product distribution of the process. Therefore in this study we analyze the effect of the zeolite structure by comparing the behavior of HZSM5 and HBeta, ( $\text{SiO}_2/\text{Al}_2\text{O}_3$  molar ratio=80 and 75, respectively) in Mo/alumina-zeolite catalysts, over the activity, selectivity and octane enhancement, during the hydroconversion of the n-heptane-methylcyclohexane-toluene model mixture.

The results of this study indicated that the main reaction pathways which produce high octane hydrocarbons over the catalysts used here were isomerization and cracking of n-heptane and methylcyclohexane, dimerization-cracking of n-heptane, and aromatic alkylation reactions.

It was also found that pore size of the zeolite has an important influence over the catalysts selectivity, thus modifying the relative importance of the main reaction paths. Since both HZSM5 and HBeta zeolites used here showed similar acid properties (pyridine FT-IR) and almost all of the structural aluminum is mainly in tetrahedral coordination (<sup>27</sup>Al-NMR) the changes observed in selectivity could be mainly associated with the different pore structure of the zeolite. While Mo/alumina-HZSM5 catalyst produces a small amount of high-octane hydrocarbons, which is mainly due to the restricted structure of HZSM5 zeolite, Mo/alumina-HBeta catalyst leads to a higher production of bulky alkyl-aromatics and di-branched isoheptanes that contribute to the octane enhancement of the product.

## 1. Introduction

It is well-known that the main objective of the hydroconversion processes is to convert hydrocarbons to a fraction with increased octane number by catalyzing reactions such as cracking, isomerization, alkylation or aromatization, avoiding at the same time catalyst decay by coke deposits (1). In the past, most hydroconversion studies were performed with single molecules like n-heptane (2). Even in these simple studies a great number of reactions take place. Not surprisingly due to the complexity of the problem, only few studies have been performed using complex feedstocks, which are more representative of the processes occurring with real feeds (3). In this case, the number of main reaction routes leading to the observed product distribution increases substantially.

For gasoline cuts, there is a growing need for high octane-low sulfur products which is mainly due to the each time more drastic environmental restrictions. Therefore it is desirable a selective hydroconversion process that allows recovering or even enhance the octane number of different gasoline cuts. The catalyst for this process needs a special design, since it will possibly work in the presence of low amounts of sulfur and nitrogen compounds, then the use of noble metals such as Pt is not the best option. However, a molybdenum metallic phase, which can work in the reduced and partially sulfided state, appears as an interesting option. The chemistry and behavior of this hydroconversion catalyst is however not well known. Only recently molybdenum has been proposed as the hydrogenating function of hydroconversion catalysts for this process (4).

Along with the previously mentioned factors, the pore size and structure of the zeolite has a crucial influence on the catalytic performance of hydroconversion catalysts (5). Small changes in either pore diameter or molecular size can change the diffusivity of alkanes by orders of magnitude (6). For example it is well-known that low octane hydrocarbons can be transformed selectively into the cavities of the HZSM5 zeolite (pore diameter  $\cong 5.4 \text{ \AA}$ ), however, the production of multibranched isomers becomes limited, which results from the restricted pore structure of this zeolite. In a recent study we analyzed the hydroconversion of a model mixture of hydrocarbons over HZSM5 based catalysts (7). The results of this study showed a scarce production of high-octane multibranched paraffins and alkylaromatics, which results from the slow diffusion of these compounds in the cavities of the HZSM5 zeolite. Therefore it is probable that the incorporation of a large pore zeolite like HBeta to the hydroconversion catalyst increases the production of high octane hydrocarbons.

The present study analyzes the hydroconversion of a complex hydrocarbon mixture constituted by a paraffin (n-heptane 70 vol.%), an aromatic (toluene, 20 vol. %) and a cycloparaffin (methylcyclohexane 10 vol.%) over presulfided Mo/alumina + zeolite catalyst. The effect of the pore size of the zeolite over the production of high-octane hydrocarbons will be analyzed by comparing the catalytic behavior of Mo/alumina-HZSM5 and Mo/alumina-HBeta catalysts. The main reaction pathways with impact on octane enhancement and liquid yield will be analyzed and discussed in terms of catalyst characterization (XRD,  $^{27}\text{Al}$ -NMR and pyridine FT-IR).

## 2. Experimental

Formulations of [Mo(x)/Al<sub>2</sub>O<sub>3</sub> + zeolite(20%)] catalysts, x=3 wt % of Mo, were prepared by physical mixing either HZSM5 or HBeta (Si/Al molar ratio= 80 and 75 respectively) and Mo/Al<sub>2</sub>O<sub>3</sub> powders. Molybdenum was supported by pore volume impregnation with aqueous solutions of (NH<sub>4</sub>)<sub>6</sub>Mo<sub>7</sub>O<sub>24</sub>·4H<sub>2</sub>O, followed by drying (373 K, 12 h) and calcination in air at 773 K. The physical mixtures were pressed at 10 Ton/cm<sup>2</sup>, and then crushed and sieved to 150 mesh.

The catalytic experiments were performed in a continuous flow tubular reactor using a feed mixture of n-Heptane (62.25 mol %)-Methylcyclohexane (10.82 mol %)-Toluene (26.86 mol %). The catalytic experiments were conducted at, T=523/688 K, P=2.8×10<sup>6</sup> Pa, and a molar hydrogen/hydrocarbon ratio of 2, these operating conditions are within the range of those reported for industrial practice (8). The LHSV used here was however smaller, LHSV of 1-10 h<sup>-1</sup>. Prior to the catalytic test, the catalysts were activated by sulfidation pretreatment. In the reaction experiments with the Mo sulfided catalysts a sulfur content of 150 ppm of S as CS<sub>2</sub>, was added to the mixture to maintain the catalyst in the sulfided form. Product analysis was performed by gas chromatography in a HP 5890-II apparatus, using a HP-PONA capillary column. The identification of reaction products was carried out with a HP G1800 GCD mass spectrometer.

The catalysts were characterized by X-ray diffraction (XRD) in a Siemens D5000 diffractometer, using Cu K $\alpha$  radiation, a goniometer speed of 1.0<sup>o</sup>/min and a graphite monochromator, in the 2<sup>o</sup> ≤ 2 $\theta$  ≤ 70<sup>o</sup> range. The <sup>27</sup>Al MASS NMR experiments were performed in a Bruker ASX300 spectrometer, using electromagnetic radiation of 56.63 MHz. FT-IR spectra were recorded on a Nicolet Magna 750 Fourier transform instrument, using pressed disks of the pure catalysts powders, activated by outgassing the IR cell at 873 K. To improve resolution, the IR experiments on the interaction of pyridine with the catalysts were performed using pure HZSM5 or HBeta zeolites. The adsorption experiments consisted of a 3 min contact of the activated catalyst with pyridine vapors (10 torr) which allowed saturating the available surface. After that, outgassing was performed. Spectra were recorded before and after outgassing.

## 3. Results and discussion

### 3.1 Catalyst characterization.

XRD analysis of HZSM5 and HBeta samples (not shown) was performed in order to verify the crystalline structure of both zeolites. It was also observed that the XRD patterns did not change after pressing the catalyst.

The <sup>27</sup>Al-NMR spectrum of the HZSM5 zeolite (Figure 1) only showed a signal at 50 ppm indicating that almost all the aluminum species were tetrahedral and located in the zeolite framework. On the other hand, the <sup>27</sup>Al-NMR spectrum of the HBeta zeolite shows a small peak around 0 ppm indicating that only a small portion of the aluminum is in octahedral coordination, the remaining aluminum species were also in tetrahedral coordination.

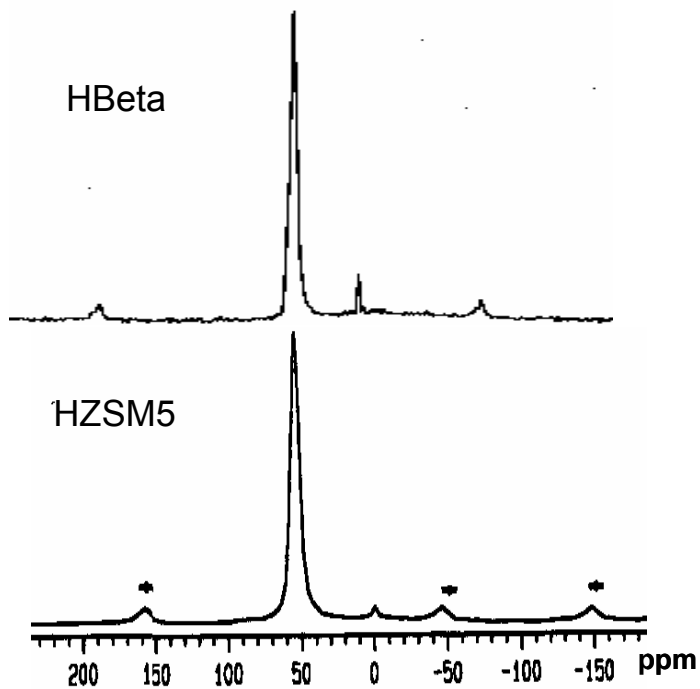


**Figure 1.**  $^{27}\text{Al}$ -NMR spectra of HZSM5 and HBeta zeolites.

The FT-IR spectra of pyridine adsorbed onto HZSM5 and HBeta zeolites at various temperatures are shown in Figure 2. Only the bending and ring-stretching frequency range is shown. The absorption bands at  $1545$  and  $1455\text{ cm}^{-1}$  are due to adsorbed pyridine ion and pyridine, respectively, as reported previously (9). Consequently the former can be related to pyridine adsorbed onto Brönsted sites and the latter to pyridine adsorbed onto Lewis sites. All other bands shown in Figure 2 were attributed on the basis of spectral variation with increasing temperature. In this figure we can also appreciate that the characteristics of the signal located around  $1545\text{ cm}^{-1}$  for both zeolites are similar, which could be explained by their similar Si/Al molar ratio.

In the case of the signal associated with the Lewis acidity ( $1455\text{ cm}^{-1}$ ), more intense bands are observed for the HBeta sample when compared with the HZSM5 counterpart. This result could be associated with the octahedrally coordinated aluminum which was detected by a small signal around  $0\text{ ppm}$  in the  $^{27}\text{Al}$ -NMR spectrum of that zeolite.

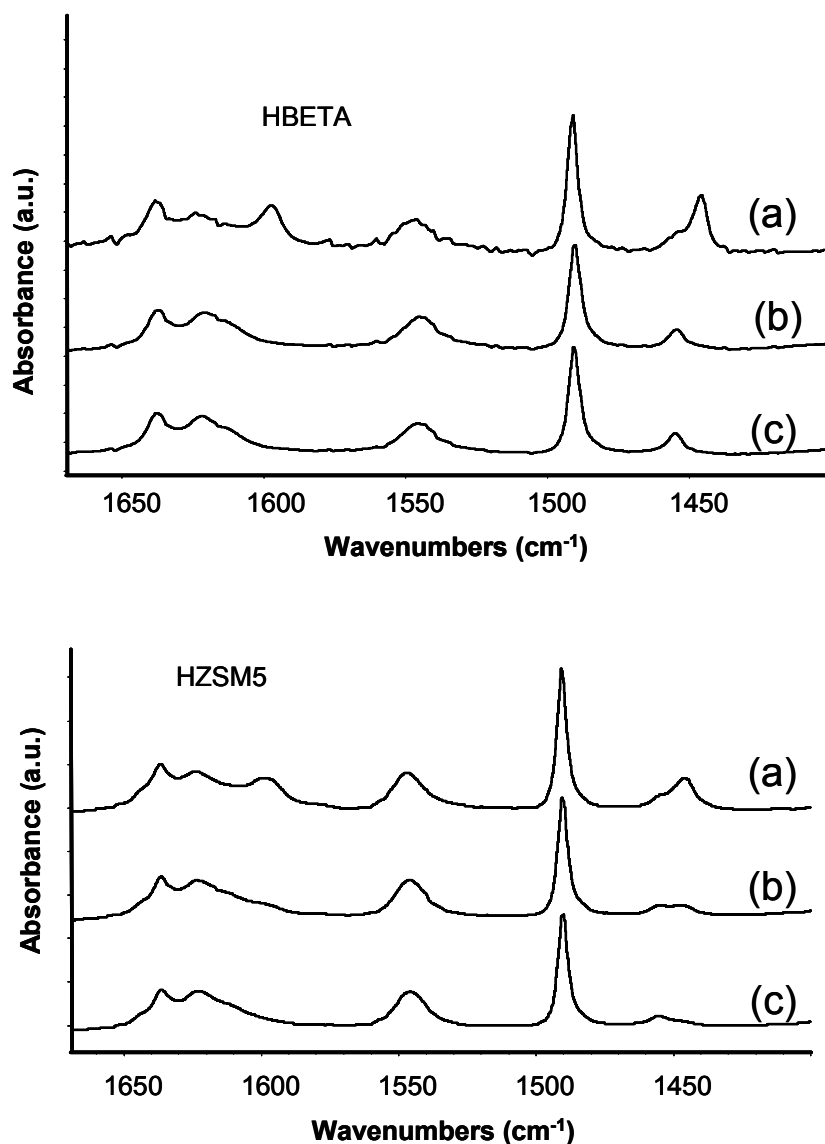


**Figure 2.** FT-IR spectra recorded after pyridine adsorption on HBeta and HZSM5, followed by evacuation at different temperatures: (a) 373, (b) 473 and (c) 573 K.

### 3.2 Hydroconversion experiments

Previous studies related to the hydroconversion of model mixtures of hydrocarbons over HZSM5 based catalysts (7, 10) have showed some experimental evidences which confirm the importance of shape selectivity effects over the production of high-octane hydrocarbons. For example, the scarce production of multibranched n-heptane isomers during n-heptane hydroconversion is mainly associated with steric constraints imposed by the small cavities of the HZSM5 zeolite. Because of these effects, in this study we analyze the changes induced by the incorporation of a large pore zeolite (HBeta) to the hydroconversion catalyst, over the production of high octane hydrocarbons.

In Table 1 the detailed product distribution obtained during the hydroconversion of the model mixture of n-heptane-methylcyclohexane-toluene over Mo/alumina-HZSM5 and Mo/alumina-HBeta is presented.

Preliminary data showed that no conversion of reactants takes place in the empty reactor or in the reactor filled with alumina. Independent experiments with Mo/alumina also showed a small production of hydrogenated aromatics and branched products (<1 mol%). Therefore, most of the acid activity was associated to the zeolite component and not to alumina.

Additional experiments carried out at the same conditions using a liquid feed containing only aromatics (i.e. pure toluene), did not give rise to significant conversion in the reactor filled with the Mo/alumina-zeolite catalyst. On the contrary, n-heptane was readily converted producing mainly gaseous light hydrocarbons with small amounts of C<sub>5</sub>, C<sub>6</sub> and C<sub>7</sub> isomers, and even smaller amounts of alkylaromatics (C<sub>8</sub> and C<sub>9</sub>). Methylcyclohexane was also converted to C<sub>7</sub>-cycloparaffins and light product, but in a lower extent than n-heptane.

The results of the hydroconversion experiments using the model mixture of n-heptane-methylcyclohexane-toluene as the feed over Mo/alumina-zeolite catalysts, show that the predominant reaction products lighter than heptane are alkanes with predominance of butane, isobutene, pentane and hexane. Only very small amounts of light olefins are detected, with predominance of butenes and 2-methyl-2-butene. Some branched n-heptane isomers and small amounts of heptenes are also found. Among the products heavier than the reactants, a clear predominance is found for alkyl-toluenes. Detectable amounts of alkanes higher than heptane (>C<sub>7</sub>) are also found, predominantly linear isomers, with only traces of branched isomers. These higher paraffins, can be the result of aliphatic alkylation reactions between olefinic fragments and carbenium ions adsorbed on the catalyst surface, both of them produced during heptane cracking.

As we can appreciate in Table 1, some important differences in product distribution exist when comparing the catalytic behavior of HZSM5 and HBeta based catalysts. The higher production of n-heptane and methylcyclohexane isomers observed when using the Mo/alumina-HBeta catalyst is the result of less drastic steric constraints imposed by the cavities of the HBeta zeolite and to the facile diffusion out of the channels of the bulky n-heptane and methylcyclohexane isomers. Another important index is the 2-methylhexane/3-methylhexane molar ratio, which took a value of 2.6 and 0.9 for HZSM5 and HBeta based catalysts respectively. The experimental values of this index indicates that the transport of 3-methylhexane (which has a higher molecular diameter than 2-methylhexane) occurs with difficulty in the cavities of the HZSM5 zeolite.

The production of dimethyl-pentanes was also increased in the cavities of the HBeta catalyst (approximately 1.7 mol%) when compared with the production observed using the HZSM5 based catalyst. In fact the percentages of 2,3-dimethylpentane and 2,4-dimethylpentane were very close to their equilibrium values at similar operating conditions. A similar behavior has been previously reported during the hydroconversion of n-heptane over MFI and MEL zeolites (11).

**Table 1.** Detailed product distribution for the hydroconversion experiments.

Catalyst	Mo/Al <sub>2</sub> O <sub>3</sub> +HZSM5	Mo/Al <sub>2</sub> O <sub>3</sub> +HBeta	Catalyst	Mo/Al <sub>2</sub> O <sub>3</sub> +HZSM5	Mo/Al <sub>2</sub> O <sub>3</sub> +HBeta
Product	mol,%	mol,%	Product	mol,%	mol,%
Light products ≤C <sub>4</sub>	8.98	9.15	Toluene	23.960	23.140
Isopentane	0.120	0.302	3-methylheptane	tr	0.040
n-pentane	0.313	0.060	n-octane	0.010	0.037
2-methyl-2-butene	0.031	0.027	Ethylbenzene	0.001	0.035
Cyclopentane	0.001	0.048	m-xylene	0.010	0.301
2,3-dimethylbutane	0.006	0.005	p-xylene	0.012	0.309
2-methylpentane	0.048	0.107	o-xylene	0.009	0.104
3-methylpentane	0.021	0.037	isopropylbenzene	0.005	0.023
n-hexane	0.215	0.045	n-propylbenzene	0.009	0.025
2,2-dimethylpentane	0.002	0.012	m-ethyltoluene	0.012	0.121
methylcyclopentane	0.016	0.286	p-ethyltoluene	0.001	0.068
2,4-dimethylpentane	0.007	0.155	o-ethyltoluene	0.001	0.026
Benzene	0.030	0.406	1,2,4-trimethylbenzene	0.005	0.015
3,3-dimethylpentane	0.003	0.012	1,2,3-trimethylbenzene	0.082	0.371
2-methylhexane	0.057	1.055	1-methyl-2-isopropylbenzene	0.003	0.031
2,3-dimethylpentane	0.010	0.112	1-methyl-4-isopropylbenzene	0.278	0.156
1,1-dimethylcyclopentane	0.003	0.095	1-methyl-3-n-propylbenzene	0.129	0.066
3-methylhexane	0.062	0.420	1-methyl-4-n-propylbenzene	0.208	0.036
c-1,3-dimethylcyclopentane	0.025	0.574	1-methyl-2-n-propylbenzene	0.008	0.018
t-1,3-dimethylcyclopentane	0.027	0.393	Dimethyl-ethylbenzenes	0.020	0.032
3-ethylpentane	0.036	0.041	tetramethylbenzenes	0.041	0.022
t-1,2-dimethylcyclopentane	0.039	0.172	non identified	0.451	0.772
C <sub>7</sub> -Olefins	0.018	0.096			
n-heptane	54.790	53.737	TOTAL	100	100
methylcyclohexane	9.885	6.905			

In a recent study the hydroconversion of n-heptane over HZSM-22, HY and HBeta zeolites was analyzed. From the results of this study it was possible to conclude that the acidity of the catalyst is a less important parameter than the structure of the zeolites (5). Therefore in our study the differences in acidity previously observed between HZSM5 and HBeta zeolites, could play a secondary role during the hydroconversion of the model mixture.

The isobutane/n-butane ( $iC_4/n-C_4$ ) molar ratio is an additional parameter which indicates the relative importance of the  $\beta$ -scission mechanisms that occur during the hydroconversion process. The experimental product distribution (Table 2) shows a higher  $iC_4/n-C_4$  ratio ( $\sim 12$ ) for the HBeta zeolite when compared with HZSM5 counterpart ( $\sim 2$ ). This result indicates that during n-heptane conversion, the cracking occurs mainly by the  $\beta$ -scission (type B) route of the dibranched isomers. On the other hand HZSM5 enhance the  $\beta$ -scission (type C) route of the monobranched isomers. Thus this result indicates in an indirect way, that the production of dibranched isomers is enhanced in the cavities of the HBeta zeolite.

The changes in selectivity induced by the incorporation of a large pore zeolite (HBeta) to the hydroconversion catalyst are reflected in a more practical way by comparing the octane number of the liquid product. It is clear from Table 2 that the production of a higher amount of n-heptane isomers and alkylaromatics leads to a higher octane number (approximately one unit) of the liquid product. Thus the incorporation of a large pore zeolite like HBeta with less drastic steric constraints to the hydroconversion catalyst, allow us to obtain a higher yield of bulky n-heptane isomers and alkylaromatics, which contribute to the octane enhancement of the liquid product.

**Table 2** Product distribution by groups, conversion of the reactants and other important indexes.

	Mo/alumina+ HZSM5	Mo/alumina +HBeta
	% mol	
C <sub>4</sub> -	8.98	9.15
C <sub>5</sub>	0.48	0.41
C <sub>6</sub>	0.57	0.90
C <sub>7</sub>	0.33	3.47
C <sub>8</sub>	0.04	0.96
C <sub>9</sub>	0.10	0.68
C <sub>10</sub>	0.68	0.36
C <sub>10</sub> +	0.17	0.27
Methylcyclohexane	9.88	6.91
n-heptane	54.79	53.74
Toluene	23.96	23.14
n-heptane conversion, %	11.9	13.7
Methylcyclohexane conversion, %	8.7	36.1
Toluene conversion, %	10.8	13.8
$iC_4/nC_4$	2.05	11.77
2-Methylhexane/3-Methylhexane	2.51	0.91
Liquid yield, %	91	90.8
RON of the liquid product	33.4	34.3



Figure 3 shows the effect of the temperature over the gain in RON, loss of liquid yield and gain in barrel octane for the Mo/alumina-HZSM5 catalyst. The former parameter ( $\Delta\text{RON}$ ) is defined as the difference between the RON of the product minus that of the feed. A similar definition is applied for the gain in barrel octane ( $\Delta\text{BO}$ ), while the loss of liquid yield is the weight percent of liquid transformed to light hydrocarbons  $\text{C}_4^-$  ( $\Delta\text{LY}$ ). We can observe that at low temperature isomerization and alkylation reactions are thermodynamically favored, therefore the gain in RON becomes more important than the loss of liquid yield giving as a consequence a net gain in barrel-octane.

At higher temperature the gain in RON is still growing, however at this operating zone the loss of liquid yield predominates over the gain in RON so the final result is a decrease of the barrel-octane of the product. It is important to remember that at high temperature cracking reactions are thermodynamically favored while isomerization and alkylation are limited. From the thermodynamic and kinetic point of view we can conclude that an intermediate operation temperature (573-603 K) is more appropriated for improving the production of high octane hydrocarbons maintaining at the same time a lower production of light products.

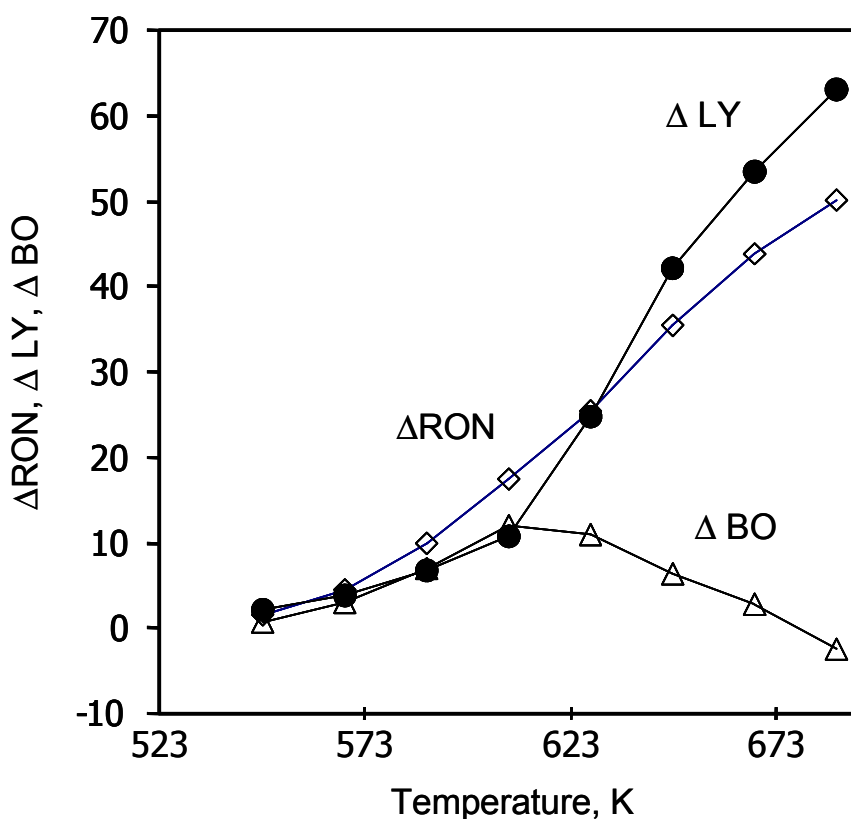


**Figure 3.** Effect of the temperature over the gain in RON ( $\Delta\text{RON}$ ), loss of liquid yield ( $\Delta\text{LY}$ ) and gain in barrel-octane ( $\Delta\text{BO}$ ).

### 3.3 Main reaction pathways

The hydroconversion of the model mixture of n-heptane-methylcyclohexane-toluene over Mo/alumina-zeolite will possibly occur through both monofunctional and bifunctional mechanisms. Here we describe the bifunctional mechanism; in this case we suppose that the Mo species are capable of catalyzing the hydrogenation-dehydrogenation reactions. In the presence of a hydrogenating function the initiation and termination steps are performed over the metallic sites, where the hydrocarbons are dehydrogenated producing olefinic compounds, following the classical hydrocracking mechanism (12). In the case of n-heptane, the olefinic intermediaries ( $O_7$ ) are isomerized over the zeolite Brönsted acid sites through a protonated cyclopropane intermediary, leading mainly to monobranched and dibranched compounds, as a result of the shape selectivity effects of the zeolite (13). Once formed, the branched n-heptane isomers are more susceptible to undergo cracking reactions over the acid sites through the conventional  $\beta$ -scission mechanism, generating new carbenium ions and short olefins ( $O_3$  and  $O_4$ ) as the main products. An alternative bimolecular cracking mechanism, called dimerization-cracking, could explain the production of  $P_5$  and  $P_6$  hydrocarbons (14). This route is carried out through an olefinic  $O_{14}$  intermediary, which after cracking produces  $O_5$  and  $O_6$  hydrocarbons without significant production of  $P_1$  and  $P_2$  products.

The transformation of methylcyclohexane yields similar products than n-heptane. Once dehydrogenated over the metallic sites, the olefinic intermediaries are protonated and isomerized on the acid sites, then, by ring contraction and ring opening some  $P_7$  branched paraffins are produced. These  $P_7$  isomers can then be transformed by pathways similar to those of n-heptane isomers. Because of this, the model considers the transformation of methylcyclohexane and n-heptane within the same lump. Below 400 °C, toluene did not react over the catalyst. However, in the presence of n-heptane, a significant increase in aromatics conversion was observed. The study shows that aromatic alkylation is produced once the intermediary olefinic compounds are formed.

The above results show that the main reactions pathways on the metallic sites are hydrogenation and dehydrogenation, which are the initiation and termination steps of the bifunctional hydroconversion process. On the acid sites isomerization and cracking of n-heptene and methylcyclohexene, and toluene alkylation reactions are the main routes. Taking into account these reaction pathways, a lumped reaction scheme is proposed in Figure 4.

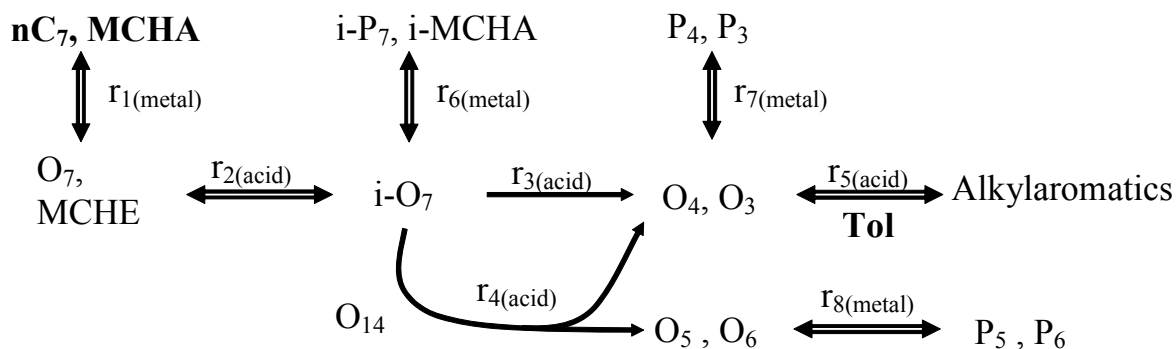


**Figure 4.** Hydroconversion of n-heptane-methylcyclohexane-toluene over Mo/alumina-zeolite catalysts. Main reaction pathways.

#### 4. Conclusions

1.- The results of this study indicated that the main reaction pathways which produce high octane hydrocarbons over the catalysts used here were isomerization and cracking of n-heptane and methylcyclohexane, dimerization-cracking of n-heptane, and aromatic alkylation reactions.

2.- The pore size of the zeolite has an important influence over the catalysts selectivity, thus modifying the relative importance of the main reaction paths. The incorporation of a large pore zeolite like HBeta with less drastic steric constraints to the hydroconversion catalyst, allow us to obtain a higher yield of bulky n-heptane isomers and alkylaromatics, which contribute to the octane enhancement of the liquid product.

3.- From the thermodynamic and kinetic point of view we can conclude that an intermediate operation temperature (573-603 K) is more appropriated for improving the production of high octane hydrocarbons maintaining at the same time a lower production of light products.

#### Acknowledgments

We acknowledge financial support from the C.I.C. (Coordinación de la Investigación Científica) U.M.S.N.H. and PROMEP-SEP programs.

#### References

- (1) Cumming, K.A.; Wojciechowski, B.W. *Catal. Rev.- Sci. Eng.* 38(1), (1996), 101.
- (2) G. E. Giannetto, G. R. Perot, M. R. Guisnet, *Ind. Eng. Chem. Prod. Res. Dev.* 25, (1986), 481.
- (3) A. Chica, A. Corma, *J. Catal.* 187, (1999), 167.
- (4) Gutiérrez A., González H., Ramírez J., Busca G. *Ind. Eng. Chem. Res.* 40, (2001), 3484-3494.
- (5) Patrigeon, A.; Benazzi, E.; Travers, Ch.; Bernhard, J.Y. *Catal. Today.*, 65, (2001), 149-155.
- (6) Chen, N. Y.; Garwood, W. E.; Dwyer, F. G. *Shape Selective Catalysis in Industrial Applications*. 2nd. Ed., Marcel Dekker, Inc., 1996.
- (7) González H., Ramírez J., Gutiérrez A., Castillo P., Cortez T., Zárate R., *Catalysis Today*, 98, 1-2, (2004), 181-191.
- (8) Shih, S. S., Keville, K. M. & Lissy, D. N. (1994). US patent. 5326462. July 5.
- (9) Barzetti T., Selli E., Mascotti D., Forni L. *J. Chem. Soc. Faraday Trans.*, 92(8), (1996), 1401-1407.

- (10) Raybaud, P.; Patriceon, A.; Toulhoat, H. *J. Catal.* 197, (2001) 98-112.
- (11) Maesen, Th. L. M.; Schenk, M.; Vlugt, T. J. H.; Smit, B. *J. Catal.*, 203, (2001), 281-291.
- (12) Weisz, P.B., *Advances in Catalysis*, 13, (1962), 137.
- (13) Olson, D. H, Kokotalio, G. T., Lawton, S. L., Meier, W. M. *Journal of Physical Chemistry*, 85, (1981), 2238-2243.
- (14) Blomsma, E., Martens, J.A., Jacobs, P.A. *Journal of Catalysis*, 159, (1996), 323-331.